Tailoring plasmon resonances in the deep-ultraviolet by size-tunable fabrication of aluminum nanostructures

Atsushi Taguchi,[1] Yuika Saito,[2,a)] Koichi Watanabe,[2] Song Yijian,[2] and Satoshi Kawata[1,2]
[1]*Nanophotonics Laboratory, RIKEN, Wako, Saitama 351-0198, Japan*
[2]*Department of Applied Physics, Osaka University, Suita, Osaka 565-0871, Japan*

(Received 6 July 2012; accepted 8 August 2012; published online 22 August 2012)

Localized surface plasmon resonances were controlled at deep-ultraviolet (DUV) wavelengths by fabricating aluminum (Al) nanostructures in a size-controllable manner. Plasmon resonances were obtained at wavelengths from near-UV down to 270 nm (4.6 eV) depending on the fabricated structure size. Such precise size control was realized by the nanosphere lithography technique combined with additional microwave heating to shrink the spaces in a close-packed monolayer of colloidal nanosphere masks. By adjusting the microwave heating time, the sizes of the Al nanostructures could be controlled from 80 nm to 50 nm without the need to use nanosphere beads of different sizes. With the outstanding controllability and versatility of the presented fabrication technique, the fabricated Al nanostructure is promising for use as a DUV plasmonic substrate, a light-harvesting platform for mediating strong light–matter interactions between UV photons and molecules placed near the metal nanostructure. © *2012 American Institute of Physics*.
[http://dx.doi.org/10.1063/1.4747489]

Metal nanostructures host localized surface plasmons—resonantly excited oscillations of free electrons at metal surfaces—when irradiated by light.[1] Localized surface plasmon resonances (LSPRs) have formed the basis of a wide range of nanophotonics research and technologies, including surface-enhanced spectroscopy and nano-imaging, ultratrace biochemical sensing, subwavelength optical waveguiding and light manipulation, and light emitters and photovoltaic cells with boosted efficiencies.[2–7] Although technological developments in these applications have predominantly focused on the visible and near-infrared (NIR) spectral range over the years, there is increasing interest in extending the technology to UV wavelengths.[8–17] A potential advantage of UV plasmons is the high photon energy that matches the electronic transition energy of many organic molecules and solids. The electronically resonant excitations of materials can be favorably combined with various spectroscopic techniques, such as Raman and fluorescence spectroscopy, which will broaden the scope of the spectroscopic applications of LSPR to include ultra-sensitive detection of DNA and proteins,[17] UV material characterization,[18] and UV nano-imaging.[14]

In order to obtain plasmon resonances in the UV, we require a metal having a negative dielectric constant at UV wavelengths with a minimal loss coefficient. Aluminum (Al) is the best and probably the only choice of material that meets this criteria. The use of Al instead of gold and silver in fabricating plasmonic nanostructures was pioneered by several groups.[10–12,19] Langhammer *et al.*[11] and Chan *et al.*[12] reported LSPR at wavelengths from the visible to near-UV by varying the size of their fabricated Al nanodiscs and nanotriangles, respectively. Ekinci *et al.* reported the first clear LSPR at deep-ultraviolet (DUV) wavelengths, with a peak at 270 nm, from 40 nm wide Al nanodiscs fabricated by extreme-ultraviolet (EUV) interference lithography using a 13.4 nm synchrotron radiation source.[13] Following these studies, the next coming challenge is to realize a localized photon source for molecular resonant excitations by developing a technique for tailoring the UV plasmon energy so that it matches the electronic resonance of the molecules of interest.

In this letter, we describe size-controlled fabrication of Al nanostructure arrays with the aim of providing direct control of the LSPR at UV wavelengths. In order to achieve ultrasmall Al nanostructures, nanosphere lithography (NSL) was used in combination with mask heating to modify the nanosphere mask morphology.[20–24] Briefly, colloidal spherical particles of polystyrene (PS) beads were self-assembled to form a hexagonal close-packed (hcp) monolayer on a quartz substrate, which was then used as a mask for metal deposition onto the substrate to produce triangular Al nanostructure arrays. Before the metal deposition, the aligned nanoparticles were thermally expanded while maintaining their alignment in the hcp monolayer. This was achieved by simple microwave heating, as discovered by Kosiorek *et al.*[24] By heating up the PS beads, the diameter of the PS beads was continuously increased while the center of the sphere remained fixed, resulting in gradual shrinking of the mask apertures surrounded by three adjacent beads. By adjusting the heating duration, the size of the aperture was continuously reduced until it became infinitesimally small, which realized seamless size reduction of the fabricated aluminum nanostructure.

The present technique overcame two major shortcomings arising with the standard NSL technique.[20,21] First, in the conventional NSL, the size of the fabricated nanostructures is spontaneously determined by the diameter of the PS beads used. This means that fabricating ultrasmall structures, which is required to achieve LSPR in the DUV, becomes technically more challenging because PS beads with a diameter of less than 200 nm are difficult to align into a uniform layer.[25] In contrast, with the present technique,

a)Electronic mail: yuika@ap.eng.osaka-u.ac.jp.

infinitesimally small structures can be produced even when relatively large PS beads are used. Using larger beads also serves to reduce unwanted lattice defects formed during the hcp-aligning process. Second, continuous tuning of the size of the structure is impossible in the conventional NSL since PS beads of limited sizes are available. The present technique provides a distinct advantage in terms of the flexibility in size control over the conventional NSL technique.

Experiments were conducted as follows. Carboxyl-functionalized PS beads of 336±8 nm diameter (Microparticles GmbH) were aligned into an hcp monolayer on a quartz substrate by spin-coating. In advance of the hcp-alignment of the PS beads, a uniform layer of PS monomer (thickness <2 nm) was preformed on the substrate surface to make the aligned beads rigidly adhere to the substrate. Without this buffer layer, we found that the hcp-aligned beads became disassembled during the microwave heating process. The buffer layer was prepared as follows: 0.05 wt. % of PS monomer was dissolved in water, and the solution was spin-coated onto the substrate. The coated PS layer was then subjected to UV irradiation using a low-pressure mercury lamp for 20 min to photochemically modify the surface. This changed the surface from hydrophobic to hydrophilic, which contributed to the adhesion of PS beads to the substrate.[25] The duration of the UV irradiation was critical for successful alignment of the PS beads, because too short UV irradiation would have caused the surface to remain hydrophobic, which would have hampered the spin-coating of PS beads, whereas overly long UV irradiation would have completely decomposed the PS polymer, with no extra bonding for the PS beads left. The surface conditions were monitored by water contact angle measurements and the best condition was found for an angle of 43°. PS beads in water solution (7 wt. %) were spin-coated onto this buffer to form self-assembled structures serving as PS masks. Using the optimal spin-coating conditions, a uniform hcp monolayer of PS beads was obtained over an area of around 20 mm × 20 mm.

The hcp-aligned PS masks were then placed in a pre-heated 50 mL solution of ethanol (boiling temperature 78.4 °C) and was continually heated in a microwave oven (Elabitax ERD-2S, 70 W, 2450 MHz). The effects of the microwave heating on the morphology of the nanosphere masks were characterized by scanning electron microscopy (SEM, JEOL SM31010, 5 keV, 12 μA) with a 3 nm-thick osmium coating to avoid unwanted charging effects. The results are shown in Figs. 1(a)–1(d) for heating times of 0 s, 90 s, 100 s, and 110 s, respectively. It was clearly observed that the size of the gaps between PS beads decreased with increasing microwave heating time. At the initial 90 s heating time, the adjacent beads became connected with each other, forming a bridge between them (from Figs. 1(a) and 1(b)). During this stage, the gap size remained relatively unchanged compared with the successive heating durations. Further increasing the heating time brought about rapid expansion of the beads, resulting in a reduced gap size (Figs. 1(c) and 1(d)). After heating for more than 130 s, we observed that the gaps were totally closed, ending up with a seamless layer of PS beads. These results demonstrate that given PS beads with a certain diameter, the size of the gap can be continuously adjusted from the initial spontaneously determined size to an infinitesimally small size by simply adjusting the microwave heating time.

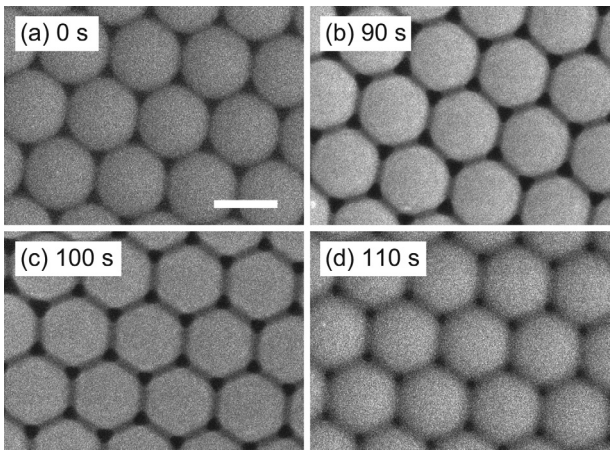

FIG. 1. SEM images demonstrating the shrinkage of the gaps between aligned PS beads upon microwave heating. The heating times were (a) 0 s, (b) 90 s, (c) 100 s, and (d) 110 s. The scale bar is 300 nm.

Next, Al (99.99% purity) was deposited onto the substrate through the prepared PS masks in a vacuum condition ($\sim 2 \times 10^{-4}$ Pa) to form Al nanostructures. The deposition thickness was set at 30 nm at a rate of 0.1 Å/s. After the deposition, the PS mask was removed by applying sonication for 30 s in water. The deposition thickness was separately checked by atomic force microscopy (AFM, SII-NT, SPA400) measurements. SEM images of the fabricated Al nanostructures produced with the masks heated for 0 s, 90 s, 100 s, and 110 s are shown in Figs. 2(a)–2(d), respectively. It is obvious that the PS beads that were heated for a longer time produced structures having smaller lateral sizes. The average widths of the fabricated nanostructures were 79.9±7.4 nm, 71.4±4.6 nm, 59.1±5.4 nm and 50.1±4.0 nm for the mask heating times of 0 s, 90 s, 100 s, and 110 s, respectively (see Table I). These results demonstrated that metal nanostructures as small as several tens of nanometers could be easily fabricated by a combination of NSL and the mask heating technique. This greatly simplifies the

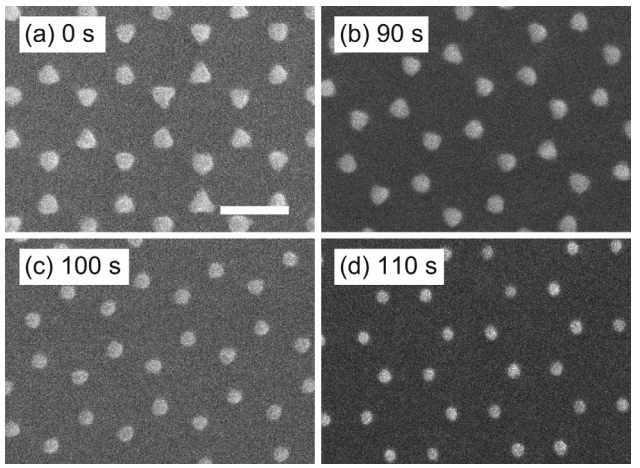

FIG. 2. SEM images of Al nanostructures fabricated using nanosphere masks heated for (a) 0 s, (b) 90 s, (c) 100 s, and (d) 110 s. The deposition thickness was 30 nm. The scale bar is 300 nm.

TABLE I. Size, circularity, and LSPR wavelength of the nanostructures fabricated with different heating times.

Heating time (s)	Width (nm)	Circularity[a]	LSPR (nm)
0	79.9±7.4	1.15±0.04	342
90	71.4±4.6	1.11±0.01	314
100	59.1±5.4	1.11±0.02	295
110	50.1±4.0	1.09±0.01	270

[a]Defined as the ratio of the square of the perimeter to $4\pi A$, where A is the area of the structure. This value is 1.654 for a regular triangle and approaches 1 for a perfect circle.

preparation of ultrasmall Al nanostructures, which currently relies on elaborate techniques such as EUV lithography.[13]

Another point we noticed from the SEM images is that the shape of the Al nanostructures gradually changed from sharp triangles to more sphere-like. Such a shape change was also observed in the shape of the gaps in the heated masks (Fig. 1) and happens along with the expansion of the beads. The effect of the shape changes was quantified by evaluating the circularities of the individual nanostructures, defined as the ratio of the square of the perimeter to $4\pi A$, where A is the area of the particular nanostructure. The circularity should be 1.654 for a regular triangle and should approach 1 for a perfect circle. The resultant values obtained by evaluating more than 30 structures for each heating time are listed in Table I. From these values, the fabricated nanostructures were not formed into a sharp triangular shape but rather formed into a circular disc. For masks with longer heating times, the produced structures had more circular shapes. Because LSPR is affected by not only the size but also the shape of the metal nanostructures, these shape changes can also contribute to the observed changes in the LSPR.

Finally, the extinction spectra of the fabricated nanostructures were measured using a UV-vis spectrophotometer (Shimadzu UV 3600). The results are shown in Fig. 3(a) by solid lines. Clear LSPR peaks were observed for all of the fabricated samples. The extinction spectra had peaks at 342 nm, 314 nm, 295 nm, and 270 nm for the Al structures obtained with the masks heated for 0 s, 90 s, 100 s, and 110 s, respectively. These results are also summarized in Table I. In Fig. 3(b), the LSPR peak wavelengths are plotted as a function of the structure's lateral size. For the samples with longer heating times, i.e., smaller Al structures, the LSPR wavelength moved toward deeper UV wavelengths. This trend is consistent with the reported LSPR characteristics observed in Al nanostructures.[11–13] The change in the LSPR peaks with respect to the lateral size of the nanostructures was almost linear. The shortest wavelength we obtained was 270 nm. We think that further reduction of the LSPR wavelength will be possible by more precisely controlling the heating durations using a microwave oven with lower power and/or by optimizing the Al deposition thickness.[26]

In order to obtain deeper insight into the observed plasmon spectra, we theoretically calculated the extinction spectra of *single* Al nanostructures with different sizes of 50 nm, 59 nm, 71 nm, and 80 nm. For the 50 nm and 59 nm-wide structures, the shapes were modeled as circular discs, whereas for the 71 nm and 80 nm-wide structures, the shapes were modeled as rounded triangular discs with corner radius of curvatures set at 30 nm. All heights were set at 30 nm, as

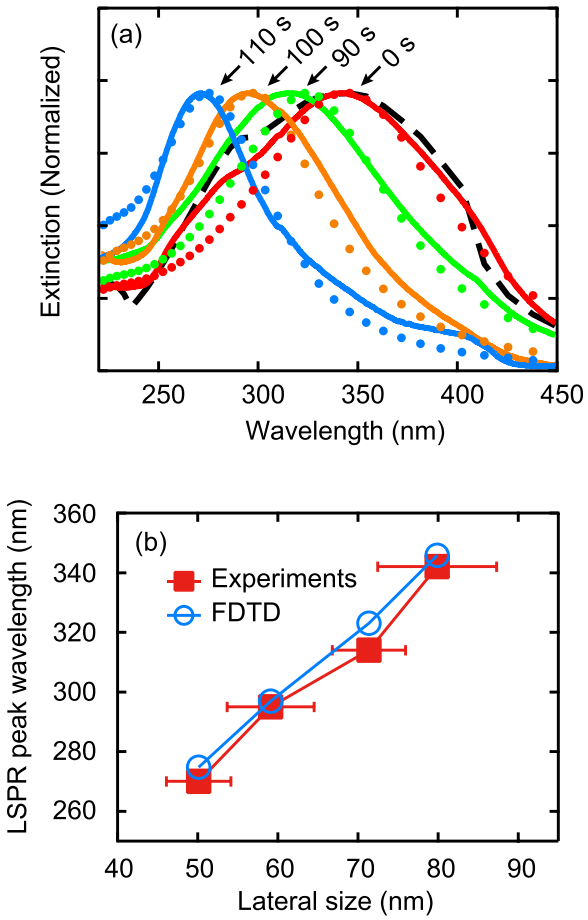

FIG. 3. (a) Extinction spectra of the Al nanostructures fabricated through PS masks with different heating times of 0 s, 90 s, 100 s, and 110 s, represented by solid lines. The spectra are normalized. The overlaid circular dots are the calculated extinction spectra of single Al nanostructures with sizes of 80 nm, 71 nm, 59 nm, and 50 nm. In the calculations, the shapes of the nanostructures were modeled as circular discs for the 50 nm and 59 nm-wide structures and as triangular discs for the 71 nm and 80 nm-wide structures, all with heights set at 30 nm. The black dashed line represents the calculated extinction spectrum for periodically aligned 80 nm nanostructures in a graphene pattern. An Al_2O_3 layer of 2 nm thickness was assumed. (b) LSPR peak wavelength vs. structure's lateral size. Experimental data are plotted in the closed squares, with the error bars representing the standard deviation of the structure's width. Theoretically calculated values are plotted in open circles.

obtained from the AFM measurements. The outermost surfaces of the models were assumed to be covered with a 2 nm-thick Al_2O_3 layer.[12] The calculations were performed using the finite-difference time-domain (FDTD) method with a mesh size of 1 nm. The calculated spectra are shown in Fig. 3(a) with circular dots, and the extracted peak wavelengths are plotted in Fig. 3(b) with open circles. There was excellent agreement of the LSPR peak wavelengths between the measured and calculated spectra. The electromagnetic field distributions at the LSPR peak wavelengths exhibited a fundamental dipole-mode-like distribution for all of the structures. In the measured spectra for the 0 s heated sample (red solid line), we observed two minor peaks at 290 nm and 400 nm, which overlapped the principal peak at 342 nm. These two peaks were also found in the other spectra at fixed spectral positions. Because the spectral positions are independent of the structure size, we think that these two peaks come from the periodicity of the fabricated nanostructures, which was fixed by the 336 nm diameter of the beads. This

idea was verified by calculating the extinction spectra for 80 nm structures aligned into a periodic graphene pattern. By incorporating the periodicity into the calculation, the two peaks were perfectly reproduced, as shown in Fig. 3(b) with a black dashed line. Aside from these peaks, the LSPR peak widths for the fundamental dipole plasmon mode were well reproduced by the theoretical calculations assuming a monodispersed size distribution. This suggests that good structural uniformity was obtained in the fabricated Al nanostructures over a wide area.

In summary, we have demonstrated control of the LSPR wavelength in the DUV region by fabricating ultrasmall Al nanostructures. Microwave heating of the aligned nanosphere masks provided a simple and cost-effective way of controlling the size of the fabricated structures. Al structures as small as 50 nm were easily obtained, and we believe that further size reduction will be possible by devising a more precise way of controlling the microwave heating duration, for example, by using microwaves with reduced power. By varying the size of Al nanostructures from 80 nm to 50 nm, the LSPR peaks were moved from 340 nm down to 270 nm. The importance of the demonstrated tunability of the LSPR energy becomes apparent when considering the use of the fabricated nanostructures as a source for molecular resonant excitations. By providing flexible size control and the capability of realizing large-scale fabrication,[22] the fabricated Al nanostructure arrays are promising for use as plasmonic substrates for UV surface-enhanced spectroscopic applications.[9,14,17]

The authors would like to thank Professor N. Zettsu at Nagoya University for helpful advice on the NSL method. This work was financially supported by JSPS Grant-in-Aid for Scientific Research (S) 21226003.

[1]C. F. Bohren and D. R. Huffman, *Absorption and Scattering of Light by Small Particles* (Wiley, New York, 1983).
[2]*Near-Field Optics and Surface Plasmon Polaritons*, edited by S. Kawata (Springer, Berlin, 2001).
[3]*Tip Enhancement*, edited by S. Kawata and V. M. Shalaev (Elsevier, Amsterdam, 2007).
[4]J. N. Anker, W. P. Hall, O. Lyandres, N. C. Shah, J. Zhao, and R. P. Van Duyne, Nat. Mater. **7**, 442 (2008).
[5]V. Giannini, A. I. Fernández-Domínguez, S. C. Heck, and S. A. Maier, Chem. Rev. **111**, 3888 (2011).
[6]N. J. Halas, S. Lal, W.-S. Chang, S. Link, and P. Nordlander, Chem. Rev. **111**, 3913 (2011).
[7]H. A. Atwater and A. Polman, Nat. Mater. **9**, 205 (2010).
[8]K. Ray, M. H. Chowdhury, and J. R. Lakowicz, Anal. Chem. **79**, 6480 (2007).
[9]T. Dörfer, M. Schmitt, and J. Popp, J. Raman Spectrosc. **38**, 1379 (2007).
[10]Y. Ekinci, H. H. Solak, and C. David, Opt Lett. **32**, 172 (2007).
[11]C. Langhammer, M. Schwind, B. Kasemo, and I. Zorić, Nano Lett. **8**, 1461 (2008).
[12]G. H. Chan, J. Zhao, G. C. Schatz, and R. P. Van Duyne, J. Phys. Chem. C **112**, 13958 (2008).
[13]Y. Ekinci, H. H. Solak, and J. F. Löffler, J. Appl. Phys. **104**, 083107 (2008).
[14]A. Taguchi, N. Hayazawa, K. Furusawa, H. Ishitobi, and S. Kawata, J. Raman Spectrosc. **40**, 1324 (2009).
[15]A. Schilling, J. Schilling, C. Reinhardt, and B. Chichkov, Appl. Phys. Lett. **95**, 121909 (2009).
[16]Z.-L. Yang, Q.-H. Li, B. Ren, and Z.-Q. Tian, Chem. Commun. **47**, 3909 (2011).
[17]S. K. Jha, Z. Ahmed, M. Agio, Y. Ekinci, and J. F. Löffler, J. Am. Chem. Soc. **134**, 1966 (2012).
[18]S. Nakashima, H. Okumura, T. Yamamoto, and R. Shimidzu, Appl. Spectrosc. **58**, 224 (2004).
[19]G. Ctistis, P. Patoka, X. Wang, K. Kempa, and M. Giersig, Nano Lett. **7**, 2926 (2007).
[20]T. R. Jensen, M. D. Malinsky, C. L. Haynes, and R. P. Van Duyne, J. Phys. Chem. B **104**, 10549 (2000).
[21]C. L. Haynes and R. P. Van Duyne, J. Phys. Chem. B **105**, 5599 (2001).
[22]J. Rybczynski, U. Ebels, and M. Giersig, Colloids Surf. A **219**, 1 (2003).
[23]A. Kosiorek, W. Kandulski, P. Chudzinski, K. Kempa, and M. Giersig, Nano Lett. **4**, 1359 (2004).
[24]A. Kosiorek, W. Kandulski, H. Glaczynska, and M. Giersig, Small **1**, 439 (2005).
[25]D. Zhang, S. M. Dougal, and M. S. Yeganeh, Langmuir **16**, 4528 (2000).
[26]J. Henson, J. DiMaria, and R. Paiella, J. Appl. Phys. **106**, 093111 (2009).